Comparison of PolSAR Speckle Filtering Techniques

Grégory Farage[1, 2]
CARTEL[1]
University of Sherbrooke
Sherbrooke, QC, Canada
gregory.farage@usherbrooke.ca

Samuel Foucher[2], Goze B. Bénié[1]
Computer Research Institute of Montreal[2]
Montreal, QC, Canada
sfoucher@crim.ca
gbenie@usherbooke.ca

Abstract— **The objective of this paper is to compare the most widely used and the most recent speckle polarimetric synthetic aperture radar (PolSAR) filters. Two new conceptual approaches in PolSAR filtering are evaluated on simulated PolSAR images. The criteria of comparison includes indicator of speckle reduction capability, edge sharpness and preservation of scattering properties. Results indicate better performances with the partial differential equation (PDE) -based filters.**

PolSAR, speckle filtering, polarimetry.

I. INTRODUCTION

The speckle noise contaminating the PolSAR data comes from the coherent nature of the SAR system. It is generated when receiving random interference of electromagnetic waves reflected by many elementary scatterers. The speckle not only affects the correlation structure between the channels: HH, VV, and HV, the three intensity images, but also the complex, cross product terms of the covariance matrix for instance. Speckle reduction enhances discrimination of scene targets by improving the accuracy of image segmentation, classification, and edge extraction [1]. However, since the polarimetric information should be preserved and the cross product adds new terms to deal with, speckle filtering is more difficult to implement in the PolSAR system than in a single polarization channel. Moreover, it is important to avoid introducing cross talking, and to keep image quality from corruption.

The first PolSAR filters were not preserving the polarimetric information, and introduced some cross talking between the channels: the polarimetric whitening filter (PWF) [2], Goze and Lopes [4] revamped the Lee et al. [3] method for one-look image, Lopes and Sery [5], and Liu et al. [6] proposed multilook PWF (MPWF).

There exist few comparisons of the relative performance of the diverse speckle filtering in the PolSAR systems. Those that have arisen recently take into account the statistical correlation and the introduction of cross talking between the channels, in order to preserve the polarimetric properties.

The recent arising of new speckle filtering techniques provides an adequate motivation to survey the most widely used and the most recent speckle filters. Assuming a stationary and multiplicative noise, the refined Lee filter [1] averages the covariance matrix in a similar way to multilook processing. The algorithm uses an edge-aligned window and applies local statistics in order to better preserve edges and spatial resolution details. The Gu et al. [7] Subspace Decomposition filter uses a high-dimensional parameter vector to characterize a pixel, and then the covariance matrix of this vector is decomposed into two subspaces: the signal subspace and the noise subspace. To end with the Subspace Decomposition methods, the reduced speckle polarimetric information is retrieved from the signal subspace. The Yu and Acton [8] speckle reducing anisotropic diffusion (SRAD) filter exploits the Partial Differential Equation (PDE) approach to regularize an image through an iterative method based on a divergence formulation for the diffusion term. In addition, this algorithm is adaptive and based on the same minimum square error approach as Lee filter. Foucher et al. [9] recently proposed the trace-based partial differential equations filter which is based on a trace based formulation for the diffusion term, and shows better preservation of the image geometric content. Lee et al. [10] also recently developed a new concept in PolSAR speckle filtering, the scattering-model-based filter that preserves the scattering mechanism of each pixel. This paper is organized as follows. In section II, we provide some background about the filtering technics to be compared. In section III, we show different results. Finally, in section IV, we compare the filtering results.

II. FILTERING TECHNIQUES FOR POLARIMETRIC DATA

In reciprocal backscattering case, $S_{hv} = S_{vh}$, polarimetric information can be represented by the scattering vector $\boldsymbol{k}_S$,

$$\mathbf{k}_S = \begin{bmatrix} S_{hh} & \sqrt{2}S_{hv} & S_{vv} \end{bmatrix}^T \quad (1)$$

where h and v represent respectively the transmitting horizontal and receiving vertical linear polarization, and the superscript "T" refers to the matrix transpose. From (1), the polarimetric covariance matrix $\mathbf{C}$ and the span are expressed as follows,

$$\mathbf{C} = \mathbf{k}_S \mathbf{k}_S^{*T} \quad (2)$$

$$span = \mathbf{k}^{*T} \mathbf{k} = |S_{hh}|^2 + 2|S_{hv}|^2 + |S_{vv}|^2 \quad (3)$$

where the superscript "*" refers to the complex conjugate.

0-7803-9510-7/06/$20.00 (c) 2006 IEEE

A. Box Filter (Mean Filter)

The box filter is a convolution filter that replaces the center pixel by the mean value of pixels in a square filtering window. Although it has a good speckle smoothing ability, it shows very poor performances in preserving spatial resolution and it alters coarsely the polarimetric parameters (entropy, coherence…). Because Box filter is an undiscriminating filter, small window sizes, 3x3 or 5x5, should be applied for filtering in order to lessen these issues.

B. Enhanced Lee Filter

The enhanced Lee filter [1] is an adaptive filter based on the estimation of the local variance statistics. The adaptive filtering weights are determined using the span image that benefits from the scattering characteristics of the HH, VV and HV intensities. The filter does not use the standard square filtering window, but an edge-aligned window with the aim of preserving edges and details features. Among eight possibilities, a non-square window is selected dependently on the edge direction detection with respect to the center pixel. The edge direction is realized by an edge mask using the submeans of 3x3 subwindows. Once the window has been chosen, the local statistics are estimated from which the local linear minimum mean-square filter is obtained,

$$\hat{x} = \bar{y} + b\left(y - \bar{y}\right) \tag{4}$$

where $\hat{x}$ is the filtered pixel value, $\bar{y}$ is the local mean, and b weighting function such as

$$b = \frac{\mathrm{var}(x)}{\mathrm{var}(y)} \quad \text{and} \quad \mathrm{var}(x) = \frac{\mathrm{var}(y) - \bar{y}^2\,\sigma_v^2}{\left(1+\sigma_v^2\right)} \tag{5}$$

where σ^2_v is the noise variance. Finally the same weight parameter b, computed from (5), is used similarly to filter each element of the covariance matrix $\boldsymbol{C}$.

C. Subspace Filter

The purpose of this technique [7] consists in decomposing in subspaces a parameter vector, which characterizes a pixel. The parameter vector $\boldsymbol{p}$ of each pixel is composed of 10 parameters. The first nine are generated from the Mueller matrix and the tenth one is the weighted entropy value. First, it is necessary to apply a square scanning window to get the local covariance matrix $\boldsymbol{C}p$ of the parameter vector,

$$\mathbf{C}_p = E\left\{\left(\mathbf{p}-\boldsymbol{\mu}_p\right)\left(\mathbf{p}-\boldsymbol{\mu}_p\right)^T\right\} = \mathbf{Q}\boldsymbol{\Lambda}\mathbf{Q}^T, \text{ and } \mathbf{Q} = \left(\mathbf{Q}_S \mid \mathbf{Q}_N\right) \tag{6}$$

where $\boldsymbol{\mu}_p$ is mean vector of the parameter vectors $\boldsymbol{p}$ in the scanning window, $\boldsymbol{Q}$ and $\boldsymbol{\Lambda}$ are respectively the eigenvectors and eigenvalues matrix of $\boldsymbol{C}p$. By assuming that there exist m (m<10) different target signals in the area to be filtered, the signal is divided in two orthogonal subspaces. The m-dimensional subspace is the "signal space" $\boldsymbol{Q}_S$, i.e the m first eigenvectors, whereas the (10-m)-dimensional subspace is called "noise subspace" $\boldsymbol{Q}_N$, which is due to speckle effect. The rank m of the "signal subspace" corresponds to the minimum number of eigenvalues required so that their sum is lager than a preset threshold η. That threshold is defined as some percentage of the sum of all the eigenvalues. Then the estimated parameter vector $\hat{\mathbf{p}}$ is rebuilt only with the "signal subspace".

$$\hat{\mathbf{p}} = \boldsymbol{\mu}_p + \mathbf{Q}_S\mathbf{Q}_S{}^T\left(\mathbf{p}-\boldsymbol{\mu}_p\right) \tag{7}$$

Finally, the filtered Mueller matrix can be extracted from the first nine elements of the estimated parameter vector.

D. Speckle Reducing Anisotropic Diffusion (SRAD) Yu Filter

The SRAD method [8] is a Partial Differential Equations (PDE) filtering algorithm that regularizes iteratively an image. During each iteration t, the image $\boldsymbol{I}$ is updated at each pixel position (x, y) according to the following PDE

$$\frac{\partial \mathbf{I}(x,y;t)}{\partial t} = \mathrm{div}\left(c(q)\nabla \mathbf{I}(x,y;t)\right) \tag{8}$$

where ∇ is the gradient operator, *div* is the divergence operator, q is the *Instantaneous Coefficient Of Variation* (ICOV)and $c()$ is the diffusion coefficient function that acts as an "edge stopping" function. The $c()$ function (9) lessen the diffusion process when ICOV becomes higher than the speckle noise level $q_0(t)$.

$$c(x,y;t) = \frac{1}{1+\left[q^2(x,y;t) - q_0^2(t)\right] \Big/ \left[\left(q_0^2(t)\right)\left(1+q_0^2(t)\right)\right]} \tag{9}$$

At each iteration, $q_0(t)$ has to be determined within an homogeneous area. The coefficient of diffusion are computed on the span and then are applied on the others elements of the polarimetric covariance matrix, or the polarimetric coherency matrix.

E. Trace Based Partial Differential Equation Filter

The trace-based [9] filter is a PDE filter that is equivalent to a local convolution by oriented Gaussian filters. The regularization process is driven by the PDE(10).

$$\frac{\partial \mathbf{I}(x,y;t)}{\partial t} = \mathrm{trace}\left(\mathbf{DH}\right) \tag{10}$$

where $\boldsymbol{D}$ is the diffusion tensor, and $\boldsymbol{H}$ is the local image hessian.

F. Scattering Model Based Filter(SMB)

The first stage of this filter [10] consists of applying a Freeman - Durden decomposition [11] on the polarimetric data. The pixels are assigned to dominant scattering mechanism category, which are one of the three: surface scattering, volume scattering, double bounce scattering mechanism. For single look images, it is necessary to realize a multilooking in azimuth until we reach an equivalent number of look of 3, otherwise an averaging window 3x3 is needed to calculate the dominant scattering mechanism. Then each set of pixels attributed to a category is divided equitably into 30 clusters, or more. Next, for each category we merge two clusters according to a merge distance measurement, until we reach n desired final classes. Afterward, all pixels are classified based on their

distance of Wishart computed with respect to the centers of classes V_m.

$$d(\mathbf{C}, \mathbf{V}_m) = \ln|\mathbf{V}_m| + Tr(\mathbf{V}_m^{-1}\mathbf{C})$$
$$\mathbf{C} \in \mathbf{V}_m \text{ if } d(\mathbf{C}, \mathbf{V}_m) \le d(\mathbf{C}, \mathbf{V}_j), \forall j \ne m \quad (11)$$

To reach a better convergence, it is preferable to apply repetitively classification of Wishart 4 times. Finally, the pixel in the center of a window of 9x9 is filtered but only using the pixels of the same class of the central pixel and the pixels which belong to two classes close to the same category. Pixels of the brightest classes for the surface and double bounce category are not filtered. Pixels belonging to the darkest or brightest classes of a category are filtered only with pixels of the same class. The filter is based on the minimization of the error quadratic, as in the enhanced Lee filter [1]. Moreover, if the quantity of pixels in filtering window 9x9 is less than 5, then we include the neighboring pixels in a 3x3 scanning window to filter.

III. RESULTS

Speckle reduction performances are evaluated on simulated PolSAR images (single look complex), produced from the Cholesky factorization [12] of typical samples polarimetric responses. Five areas with different scattering properties are selected within an E-SAR image (L-band, DLR, Oberpfaffenhofen area). The final PolSAR image $\boldsymbol{I}^{GT}$ is shown on Fig.3, as well as the ground truth image. We evaluate the performances of the PolSAR image $\boldsymbol{I}$ filtering on its three power bands with the following indicator:

- *Equivalent number of looks* (ENL): a measure that indicates the strength of the noise reduction; we compute the ENL for each power channel and each scattering classes (we exclude point targets) and we took the mean value.

$$ENL = \frac{1}{3\times 5}\sum_{n=1,2,3}\sum_{l=1,..,5}\frac{E\left[(I_n - < I_n >)^2 \mid l\right]}{< I_n >^2} \quad (12)$$

- *Edge strength preservation* (EP): preservation of the edge magnitudes of filtered image is compared to the ground truth image (the smaller the EP the more significant it is).

$$EP = \frac{1}{3\times 5}\sum_{n=1,...,3}\sum_{l=1,...,5}\left|1 - \frac{\sum_{\mathbf{x}\in Edges}\|\nabla I_n(\mathbf{x})\|}{\sum_{\mathbf{x}\in Edges}\|\nabla I_n^{GT}(\mathbf{x})\|}\right| \quad (13)$$

In addition to EP and ENL, the Table 1 presents the rate of the Entropy-Alpha classification (HA) and the Classification of the dominant scattering mechanism based on Freeman Durden decomposition (FD), shown in Fig.1. The box filter uses a 5x5 window, and for enhanced Lee a 9x9 windows. The parameters of the subspace filter are a 7x7 covariance window, a threshold of 0.8 and entropy, weighted by 6, was computed with a 7x7 averaging window. The SRAD filter run with a time step size of 0.05 during 2000 iterations, whereas the trace based filter run with a step of 0.1 during 200 iterations. The SMB filter used a 9x9 window, with 5 classes for the volume and the surface and 3 classes and 4 iterations.

TABLE I. FILTERING PERFORMANCES.

Filter	ENL [min -max]	EP [min -max]	HA (%)	FD (%)
Box	24.9 [23.8-27.7]	0.557 [0.547-0.562]	71.83	80.88
Enhanced Lee	16.7 [0.1-40.5]	0.508 [0.502-0.510]	81.80	69.24
Subspace	6.7 [0.4-14-9]	0.150 [0.116-0.209]	62.83	57.63
SRAD	91.9 [14.3-299.9]	0.070 [0.066-0.074]	91.84	82.52
Trace-Based	59.8 [26.8-79.6]	0.043 [0.037-0.059]	85.15	72.71
SMB	6.0 [1.8-30.1]	0.011 [0.004-0.022]	63.02	66.51

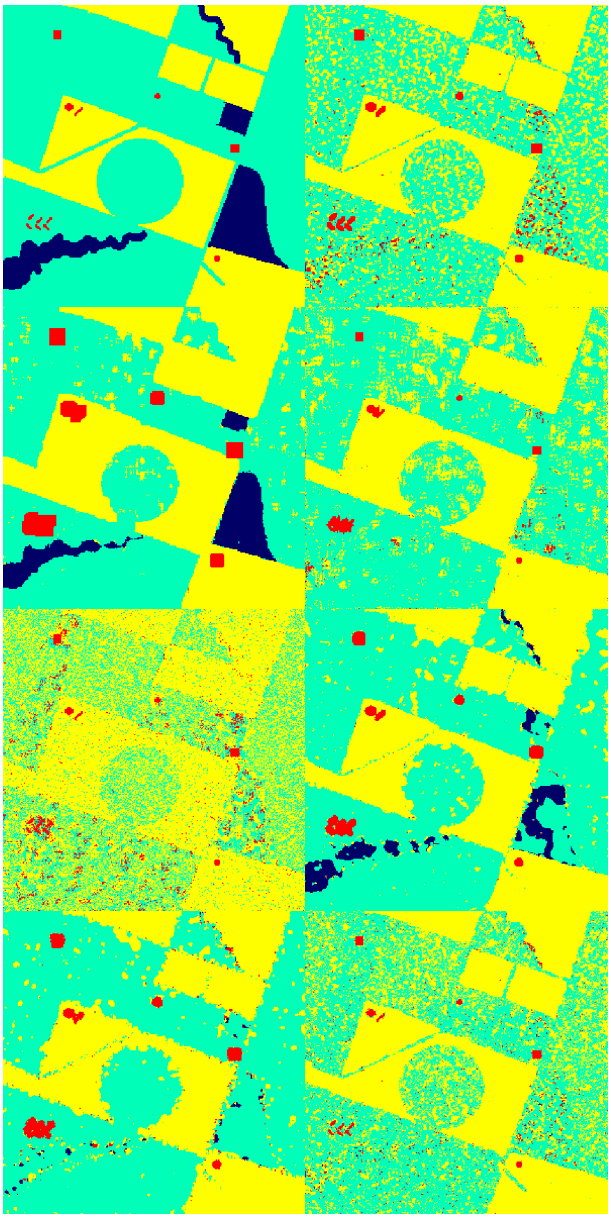

Figure 1. Classification of the dominant scattering mechanism based on Freeman Durden Decomposition, blue = undertemined, green = surface, yellow = volume, red = double bounce, and from left to right and top to bottom : ground truth, original image, box filter, enhanced Lee, Subspace, Yu, Trace, SMB.

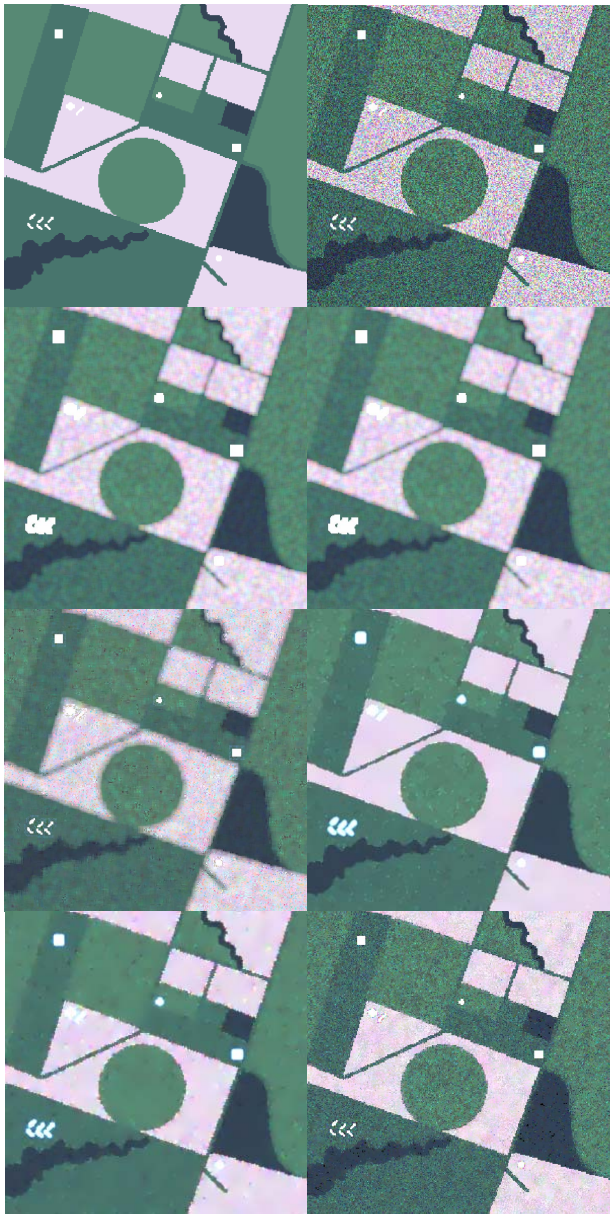

Figure 2. Span display color, red = $\sqrt{2}$ $|Shv|^2$, green = $|Svv|^2$, blue = $|Shh|^2$, and from left to right and top to bottom : ground truth, original image, box filter, enhaced Lee, Subspace, Yu, Trace, SMB.

IV. Discussion and Conclusion

The SRAD filter presents the best overall score (Table 1). It has the highest ENL value and the most accurate percentage of good classification. But compared with the trace-based filter, it has a weaker EP. We can notice from Fig.2, that SRAD filter enlarges and distorts the targets, the same applies to the Box and Lee filter. The Subspace filter succeeds to keep the target size, but neighboring pixels are altered due to the entropy parameter that has lower spatial resolution. The SMB filter possesses the best edge preservation characteristic; however it is difficult to compare this filter with the others due to its new filtering concept that aims at preserving the scattering properties. The weak ENL value of SMB could be explained by its restrictive pattern of selecting neighboring pixels. The ideal speckle filter should not only reduce speckle noise and retain meaningful spatial features, but it should also preserve the polarimetric information by avoiding cross talking between channels and mixing pixels with different scattering mechanisms. According to the set of criteria to compare speckle filtering algorithms, the PDE-based filters appear to be very efficient, while the SMB is very good at preserving point targets signature. algorithms, the PDE-based filters appear to be very efficient, while the SMB is very good at preserving point targets signature.

Acknowledgment

This work has been supported in part by the NSERC of Canada (Discovery Grant) and the MDEIE of the "Gouvernement du Québec". The authors wish to thank the DLR (German Aerospace Center) for so graciously providing them with the E-SAR dataset.

References

[1] J.S. Lee, M. R. Grunes, and G. De Grandi, "Polarimetric SAR Speckle Filtering and its Implication for Classification", *IEEE Trans. Geosci. Remote Sensing*, Vol. 37, No 5, pp 2363-2373, Sep. 1999.

[2] L.M. Novak and M.C. Burl, "Optimal speckle reduction in polarimetric SAR imagery", *IEEE Trans. Aerosp. Electron. Syst.*, Vol. 26, No 2, pp. 293-305, Mar. 1990.

[3] J.S. Lee, M. R. Grunes, and S.A. Mango, "Speckle reduction in multipolarization and multifrequency SAR imagery", *IEEE Trans. Geosci. Remote Sensing*, Vol. 29, No 4, pp 535-544, Jul. 1991.

[4] S. Goze and A. Lopes, "A MMSE speckle filter for full resolution SAR polarimetric data", *J. Electron. Waves Appl.*, Vol. 7, No. 5, pp. 717-737, 1993.

[5] A. Lopes and F. Sery, "Optimal speckle reduction for product model in multilook polarimetric SAR imagery and the wishart distribution", *IEEE Trans. Geosci. Remote Sensing*, Vol. 35, No. 3, pp. 632-647, May 1997.

[6] G. Liu, S. Huang, A. Torre, and F. Rubertone, "The multilook polarimetric whitening filter for intensity speckle reduction in polarimetric SAR images", *IEEE Trans. Geosci. Remote Sensing*, Vol. 36, No. 3, pp. 1016-1020, May 1998].

[7] J. Gu, J. Yang, H. Zhang, Y. Peng, C. Wang, and H. Zhang, "Speckle Filtering in Polarimetric SAR Data Based on the Subspace Decomposition", *IEEE Trans. Geosci. Remote Sensing*, Vol. 42, No. 8, pp. 1635-1641, Aug. 2004.

[8] Y. Yu and S. T. Acton, "Speckle Reducing Anisotropic Diffusion", *IEEE Trans. Geosci. Remote Sensing*, Vol. 11, No. 11, pp. 1260-1270, Nov. 2002.

[9] S. Foucher, G. Farage and G.B. Bénié, "Speckle Filtering of PolSAR and PolInSAR Images using Trace-Based Partial Differential Equations", *IGARSS*, Denver, Colorado, United-States, 2006, to appear.

[10] J.S. Lee, M. R. Grunes, D.L. Schuler, E. Pottier, and L. Ferro-Famil, "Scattering-modeled-based speckle filtering of polarimetric SAR data", *IEEE Trans. Geosci. Remote Sensing*, Vol. 44, No 1, pp 176-186, Jan. 2006.

[11] A. Freeman and S. L. Durden, "A three-component scattering model for polarimetric SAR data", *IEEE Trans. Geosci. Remote Sensing*, vol. 32, no. 3, pp. 1017-1028, Sept. 1994.

[12] L. Pipia and X. Fàbregas, "Generation of Pol-SAR and Pol-In-SAR Data for Homogeneous Distributed Targets Simulation", In *Workshop on Polarimetric Synthetic Aperture Radar* (ESA SP-529), Frascati, Italy, 2005.